Blockade of Annexin A2 Prevents Early Microvasculopathy in Murine Models of Diabetic Retinopathy

Valentina Dallacasagrande,[1] Wei Liu,[1,*] Dena Almeida,[1] Min Luo,[1] and Katherine A. Hajjar[1,2]

[1]Department of Pediatrics, Weill Cornell Medicine, New York, New York, United States
[2]Department of Medicine, Weill Cornell Medicine, New York, New York, United States

Correspondence: Katherine A. Hajjar, Department of Pediatrics, Weill Cornell Medicine, 1300 York Ave – Box 45, New York, NY 10065, USA; khajjar@med.cornell.edu.

Current affiliation: *Betta Pharmaceuticals Co., Ltd.

Received: November 21, 2022
Accepted: March 21, 2023
Published: April 27, 2023

Citation: Dallacasagrande V, Liu W, Almeida D, Luo M, Hajjar KA. Blockade of annexin A2 prevents early microvasculopathy in murine models of diabetic retinopathy. *Invest Ophthalmol Vis Sci.* 2023;64(4):33. https://doi.org/10.1167/iovs.64.4.33

Purpose. We examined the role of annexin A2 (A2) in the development of diabetic retinal vasculopathy by testing the effect of *Anxa2* gene deletion as well as administration of anti-A2 antibodies on pericyte dropout and retinal neovascularization in diabetic Akita mice, and in mice subjected to oxygen-induced retinopathy.

Methods. We analyzed diabetic $Ins2^{AKITA}$ mice with or without global deletion of *Anxa2*, as well as $Ins2^{AKITA}$ mice that received intravitreal anti-A2 IgG or control antibody at 2, 4, and 6 months, for retinal pericyte dropout at 7 months of age. In addition, we assessed the effect of intravitreal anti-A2 on oxygen-induced retinopathy (OIR) in neonatal mice by quantifying retinal neovascular and vaso-obliterative area, and by enumeration of neovascular tufts.

Results. Both deletion of the *Anxa2* gene and immunologic blockade of A2 prevented pericyte depletion in retinas of diabetic $Ins2^{AKITA}$ mice. Blockade of A2 also reduced vaso-obliteration and neovascularization in the OIR model of vascular proliferation. This effect was amplified when a combination of antivascular endothelial growth factor (VEGF) and anti-A2 antibodies was used.

Conclusions. Therapeutic approaches that target A2, alone or in combination with anti-VEGF therapy, are effective in mice, and may also curtail the progression of retinal vascular disease in humans with diabetes.

Keywords: annexin A2, neovascularization, retinal pericytes

Diabetic retinopathy (DR) is the most common cause of moderate and severe vision loss in working-age adults.[1] In 2020, the global prevalence of DR was 22.27% among individuals with diabetes.[2] It is further estimated that by 2045 the global population of diabetics will reach 693.0 million,[3] over 160 million of whom will have DR.[2]

The pathogenic mechanisms associated with DR are complex.[4–8] They include hyperglycemia-associated metabolic abnormalities, such as activation of protein kinase C (PKC), accumulation of polyols and glycation end products, and increased flux through the hexosamine pathway, all of which lead to production of reactive oxygen species, and damage the retinal neurovascular unit composed of endothelial cells, pericytes, glial cells, and neuronal processes. Upregulation of intercellular adhesion molecule-1 (ICAM-1) in the diabetic retina, moreover, causes accumulation of leukocytes around the vascular wall,[9] induction of a low-grade inflammatory state, loss of neurovascular coupling, and weakened tight junctions with pericyte loss and vascular leak. Subsequent hypoperfusion leads to microaneurysm formation and local ischemia, followed by upregulation of pro-angiogenic mediators, such as vascular endothelial growth factor (VEGF), erythropoietin, and angiopoietin. Together, these changes lead to proliferation of new, abnormal retinal blood vessels.

The annexin A2 complex (A2) is an endothelial cell-surface heterotetramer, consisting of 2 copies of A2 and 2 of its partner protein, S100A10 (aka p11). It serves as a co-receptor for two fibrinolytic proteins, plasminogen, and tissue plasminogen activator, and accelerates the activation of the serine protease, plasmin, initiating an activation cascade for downstream proteases, such as matrix metalloproteinases (MMPs).[10] We showed previously that A2 deficient ($Anxa2^{-/-}$) mice display reduced neovascularization in the fibroblast growth factor-stimulated cornea, and in the VEGF-driven Matrigel plug assay.[10] In addition, we found that neonatal $Anxa2^{-/-}$ mice exhibited markedly reduced retinal neovascularization (30–50%) in the oxygen-induced retinopathy (OIR) model of proliferative DR,[11] and that the *Anxa2* gene is upregulated directly by hypoxia-inducible factor-1 (HIF-1),[11] expression of which is elevated in DR.[12,13] In a choroidal neoangiogenesis model, moreover, pharmacologic blockade of A2 suppressed neovascularization.[14] Together, these studies suggest a central role for A2 in the development of ocular vascular proliferative disorders, and we, therefore, tested the ability of anti-A2 antibodies to prevent early vascular changes in 2 distinct mouse models of DR. We show that intravitreal administration of anti-A2 IgG can prevent pericyte loss, reduce pathologic neovascularization, and preserve normal retinal architecture.

Materials and Methods

Mice

All animals were housed in a 12/12-hour light/dark cycle room with free access to food and water. All animal procedures were approved by the Institutional Animal Care and Use Committee of Weill Cornell Medical College.

For the OIR model, we used the 129 strain, which exhibits more robust angiogenesis in comparison to many other strains.[11,15,16] Anxa2$^{-/-}$ and Anxa2$^{+/+}$ mice were bred as homozygotes and genotyped as described using oligonucleotides A2WT (5′-GCA, CAG, CAA, TTC, ATC, ACA, CTA, ATG,TCT, TCT, TG-3′), A2KO (5′-GCT, GAC,TCT, AGA,GGA,TCC,CC-3′), and Anint2 (5′-TGC, GCC, ACC, ACG, CCC, GGC, TTG, TGC, TTG, CCA, C-3′), resulting in a 221-bp Anxa2$^{-/-}$ band versus a 304-bp Anxa2$^{+/+}$ band.[10]

For diabetic mouse experiments, Ins2^{AKITA} mice (Jackson Labs, cat. #003548) were intercrossed for at least five generations with Anxa2$^{+/+}$ and Anxa2$^{-/-}$ C57BL/6 mice to generate Anxa2$^{+/+}$:Ins2^{AKITA} and Anxa2$^{-/-}$:Ins2^{AKITA} strains. Ins2^{AKITA} mice were maintained as heterozygotes, as homozygous Ins2^{AKITA} are known to be inefficient breeders. Ins2^{Akita} mice were genotyped according to Jackson Labs protocol #176. Briefly, PCR was conducted using oligonucleotides oIMR1093 (5′- TGC, TGA, TGC, CCT, GGC, CTG, CT-3′) and oIMR1094 (5′-TGG, TCC, CAC, ATA, TGC, ACA, TG-3′), and the products digested with Fnu4HI, resulting in a 280- versus 140-bp band in Ins2^{Akita} versus wild type mice.[17,18] Examples of Anxa2$^{+/+}$:Ins2^{AKITA} and Anxa2$^{-/-}$:Ins2^{AKITA} genotyping are included in Supplementary Figure S1.

Phenotypic analysis of Akita mice was assessed by blood glucose assay using a commercial fluorometric assay (Abcam cat. #65333), according to the manufacturer's instructions (Supplementary Fig. S2). Mean values for Anxa2$^{+/+}$:Ins2^{WT}, Anxa2$^{+/+}$:Ins2^{AKITA}, Anxa2$^{-/-}$:Ins2^{WT}, and Anxa2$^{-/-}$:Ins2^{AKITA} were 228.3 ± 11.9, 726.2 ± 24.1, 258.1 ± 15.8, and 695.2 ± 17.5 mg/dL, respectively, in agreement with published reports.[19,20]

For evaluation of pericyte dropout and retinal neovascularization, we used male mice, as female Akita mice have more inconsistent and milder diabetes, two to three-fold lower glucose levels, less organ system involvement, and longer survival times.[17,19,20]

Assessment of Pericyte Dropout

Retinas from 7-month-old wild type (*Anxa2*$^{+/+}$), *Ins2*^{AKITA}*:Anxa2*$^{+/+}$, *Anxa2*$^{-/-}$, *or Ins2*^{AKITA}*:Anxa2*$^{-/-}$ mice were isolated, fixed overnight in 4% PFA, subjected to limited ,trypsin digestion, and stained with periodic acid-Schiff (Sigma-Aldrich, Procedure 395) as described (Supplementary Fig. S3).[21] For anti-A2 treatment of wild type and Akita mice, the pupil was dilated (1% tropicamide and 2.5% phenylephrine) under systemic (isoflurane) and topical (0.5% proparacaine HCl) anesthesia. After proptosing the globe, 3 µL of PBS containing monoclonal anti-A2 (1A7, 5 µg/mL [33 nM] or 2E6, 15 µg/mL [100 nM], or a nonreactive control (1D4 15 µg/mL [100 nM]) and/or anti-VEGF-A (BioLegend 2G11-2A05, 1 mg/mL [6.7 mM]) were injected at the limbus into the vitreous using a 10-µL NanoFil syringe (WPI) and 30-gauge needle under microscopic control. Optimal doses for each antibody were determined in preliminary experiments. Antibiotic ointment was applied to the injected eye. Four fields (40 × objective) were analyzed for each retina, and the pericyte to endothelial cell (PC/EC) ratio calculated.

Oxygen-Induced Retinopathy

OIR was induced as previously described.[11] On postnatal day 12 (P12), pups were returned to room air and given an intravitreal injection of anti-A2 in the left eye under systemic and local anesthesia as described above, except that the injected volume was 1 µL via 10-µL Hamilton syringe and 34-gauge needle. Mouse retinas were isolated at P17, and processed for assessment of the neovascular (NV) area. To quantify NV and vaso-obliteration (VO) area, retinas were stained and analyzed as described.[22] For each animal, the percent VO and NV in the injected eye (OS) was normalized to the contralateral non-injected eye (OD) to calculate the relative VO and NV.

For enumeration of tuft nuclei, P17 eyes were fixed in Davidson's reagent (4°C, for 18 hours) and embedded in paraffin with the cornea and optic nerve on the same focal plane. Peripheral sections were stained with RITC GSL Lectin (Vector Laboratories, RL-1102-2) to visualize endothelial cells and DAPI to mark nuclei, and were imaged under fluorescent illumination (Zeiss Axio Imager Z1; 20 × objective). Tuft nuclei were enumerated per section and averaged for each animal.

Analysis of Human Retinas

Human eyes from de-identified, deceased donors were provided within 24 hours postmortem by the Eye Bank for Sight Restoration, Inc. (New York, NY, USA) without specific delineation of the severity or duration of diabetes, presence or duration of DR, medications, or other comorbidities. For cryostat section preparation, whole eyes were fixed (4% PFA, for 18 hours), the cornea removed, and the tissue cryoprotected (30% sucrose, 50 mM glycine in PBSCM; for 18 hours). The vitreous was then removed, and the eye infiltrated with 30% sucrose and optimal cutting temperature medium (OCT; 1:2, v:v; for 30 minutes), and frozen in liquid nitrogen. For immunofluorescence staining, cryostat sections were incubated in methanol (-20°C, for 10 minutes), and then treated to remove RPE pigment by adding removal buffer (4.7% deionized formamide, 1X sodium chloride sodium citrate buffer, and 2% hydrogen peroxide) and positioning the section at 5 inches from a light source (for 5-20 minutes). The sections were blocked with 5% species-specific normal serum (21°C, for 20 minutes), and incubated with primary anti-A2 (18 hours, 4°C or 37°C, for 90 minutes; Invitrogen, 03-4400), followed by secondary antibodies (37°C, for 30 minutes) and DAPI. For paired eyes from a given donor, one eye was used for biochemical and molecular analyses, and the other for immunohistochemical evaluation.

Western Blot Analysis

One quarter of the human retinal tissue was homogenized in RIPA buffer (50 mM Tris, pH 7.5; 150 mM NaCl, 1 mM EDTA, 1% sodium deoxycholate, and 1% NP-400 containing protease and phosphatase inhibitors [Roche, 04693159001 and 04906837001]). The protein concentration in the whole tissue extract (17,900 g, 4°C, for 10 minutes in supernatant) was determined by Bio-Rad Protein Assay. Proteins were resolved on 4% to 20% Novex tris-glycine gels (Invitrogen, XPO4200BOX) and probed for annexin

A2, p11, and pan-cadherin. Band density from at least two independent immunoblots were quantified using ImageJ software.

Plasmin Generation Assay

Microtiter plates were coated with recombinant human annexin A2 (10 µg/mL in 100 mM carbonate buffer [pH 9.6], 18 hours, 4°C). After washing thrice with 0.05% Tween-20 in PBS-CM, the plate was blocked (1.5% BSA, 0.05% Tween-20 in PBS-CM; for 1 hour at 21°C), incubated with monoclonal antibodies (0.1-50 µg/mL in blocking buffer, for 1 hour at 21°C), incubated with human glu-plasminogen in blocking buffer (170 nM, Biomedica Diagnostics, for 1 hour at 4°C), and then incubated with tissue plasminogen activator (tPA, 100 µL, 40 nM, Molecular Innovations) together with AFC-081 (125 µM, Echelon Bioscience, 872-22) in 0.2% BSA/PBS-CM. Fluorescence at 400 nm excitation and 505 nm emission was recorded using a plate fluorometer (Synergy H1, BioTek; 37°C, at 3 minute intervals). The rate of plasmin generation was calculated as the slope of the curve (RFU/min^2).

Results

Deletion of Annexin A2 Prevents Pericyte Dropout in Diabetic Akita Mice

The retina contains the highest concentration of pericytes of any vascular bed, and pericyte dropout is the earliest demonstrable vascular change in DR.[23,24] The ratio of retinal pericytes to endothelial cells (PC/EC) in non-diabetic humans is nearly 1:1, but drops to 1:4 in patients with diabetes.[25] To examine the effect of A2 expression on pericyte retention, we performed limited trypsin digestion of en face preparations of whole retinas from wild type mice (*Anxa2*$^{+/+}$); annexin A2 deficient mice (*Anxa2*$^{-/-}$); non-obese, insulin-deficient, diabetic Akita mice (*Anxa2*$^{+/+}$:*Ins2*^{AKITA}); and Akita mice cross-bred to A2-deficient mice (*Anxa2*$^{-/-}$:*Ins2*^{AKITA}). We enumerated ECs and PCs using standardized imaging at 7 months of life (see Supplementary Fig. S3) and calculated the PC/EC ratio[21] (Fig. 1). Whereas the PC/EC ratio in wild type mice was 0.3 (0.2999 ± 0.0058 mean ± SEM, n = 30 fields), the ratio dropped significantly in Akita mice (0.2186 ± 0.0050 mean ± SEM, n = 15 fields; P value < 0.0001). A2-deficient mice showed a PC/EC ratio identical to that of wild type controls (0.2996 ± 0.0122 mean ± SEM, n = 27 fields). However, unlike Akita mice on the wild-type background, Akita mice cross-bred to A2-deficient mice (*Anxa2*$^{+/+}$: *Ins2*^{AKITA}) showed no loss of pericytes, with a PC/EC ratio (0.3048 ± 0.0057 mean ± SEM, n = 35 fields) that did not differ from that of non-diabetic wild type (*Anxa2*$^{+/+}$) or A2-deficient (*Anxa2*$^{-/-}$) mice. These data revealed that expression of annexin A2 is required for early dropout of pericytes in the Akita diabetic mouse.

Blockade of Annexin A2 Reduces Pericyte Dropout in Diabetic Akita Mice

We next developed antibodies designed to inhibit annexin A2- and tissue plasminogen activator (tPA)-dependent plasmin generation in a purified protein system (Fig. 2). We tested two anti-A2 antibodies directed against the same amino terminal domain of annexin A2, as well as a third non-reactive IgG produced in the same manner. When added to A2-coated microtiter wells prior to addition of plasminogen and tissue plasminogen activator, both anti-A2 antibodies (1A7 and 2E6; see Figs. 2A, 2B) blocked the initial rate of A2-dependent plasmin generation in a concentration-dependent manner, resulting in inhibition of up to 73% (see Figs. 2A, 2B). On the other hand, the non-reactive, negative control antibody (1D4), showed no blocking activity at all (Fig. 2C). These data indicated that antibodies directed against A2 can prevent tPA-dependent plasmin generation in vitro.

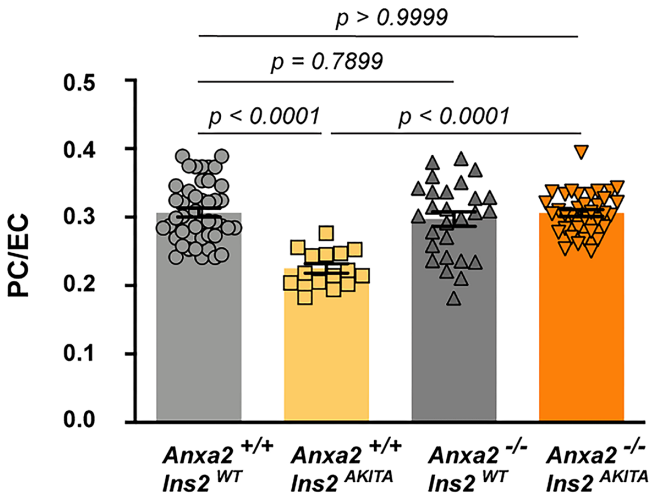

Figure 1. Effect of annexin A2 deletion on pericyte drop out in diabetic Akita mouse retinas. Pericyte cells (PCs) and endothelial cells (ECs) were enumerated in flat mount preparations of retinas following limited trypsin digestion. Four fields (40 times magnification) from a single retina from each of four to eleven animals were analyzed, each symbol representing one field. Shown are mean values for each group, derived using ANOVA and the Tukey multiple comparisons test, and SEM.

Because we observed a 40% to 60% increase in total A2 expression and a doubling of steady-state A2 mRNA in retinas from Akita diabetic mice compared to control mice (Supplementary Figs. S4A, S4B, respectively), we hypothesized that elevated A2 expression in the diabetic retina might promote retinal vasculopathy. We, therefore, tested the effect of anti-A2 antibodies on retinal pericyte dropout in the Akita diabetic mouse (Fig. 3). Both Akita and wild type mice received 3 intravitreal injections of 1A7 (15 ng), 2E6 (45 ng), or 1D4 (45 ng) at 2, 4, and 6 months of age. Antibody 1A7 had no effect on the PC/EC ratio in *Anxa2*$^{+/+}$ mice at 7 months of age (treated 0.2931 ± 0.0081 SD, n =12 fields versus untreated 0.2891 ± 0.0072 SEM, n =12 fields). However, administration of 1A7 to diabetic mice was associated with a striking preservation of the PC/EC ratio (*Anxa2*$^{+/+}$: *Ins2*^{AKITA} 0.3171 ± 0.0066 SEM, n = 10 fields) compared to untreated controls (0.2556 ± 0.0067 SEM, n = 11 fields; see Fig. 3A). Antibody 2E6 showed a similar, statistically significant effect; untreated *Anxa2*$^{+/+}$:*Ins2*^{AKITA} mice displayed a PC/EC ratio of 0.207 ± 0.0088 (SEM, n = 13 fields), which rose to 0.281 ± 0.0014 (SEM, n = 12 fields) upon antibody treatment (see Fig. 3B). At the same time, the inactive control (1D4) had no effect on pericyte dropout in either genotype (see Fig. 3C). These results revealed that functional blockade of A2 can prevent loss of pericytes in the retinas of diabetic *Ins2*^{AKITA} mice.

Investigative Ophthalmology & Visual Science

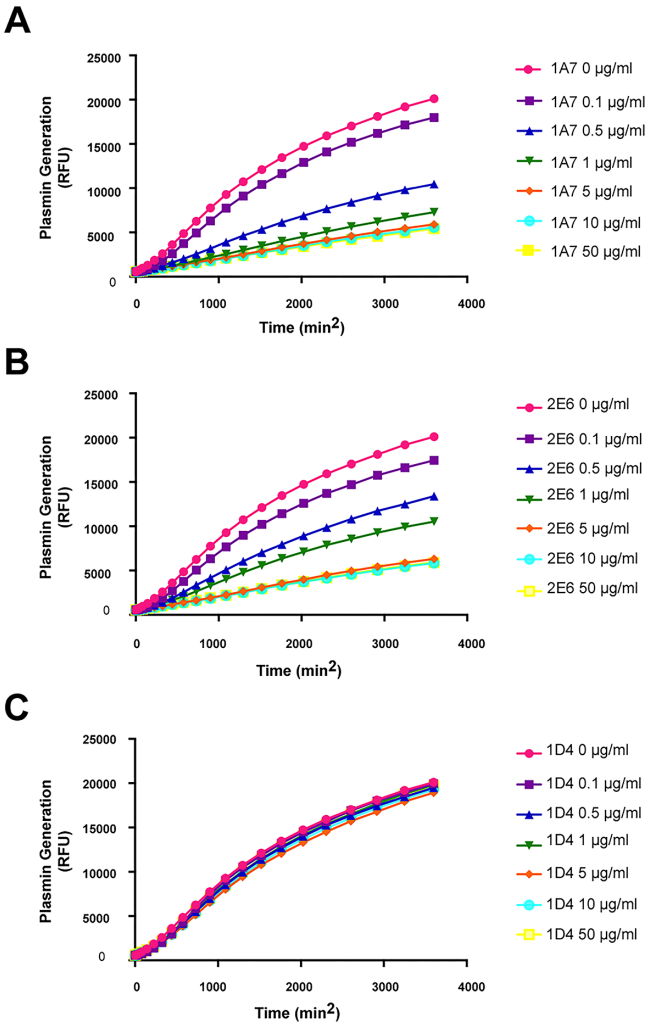

Figure 2. Effect of anti-A2 antibodies on plasmin generation in a purified protein system. Anti-A2 1A7 (**A**), 2E6 (**B**), or control 1D4 IgG (**C**), were added to A2-coated microtiter plate wells in a range of concentrations prior to incubation with plasminogen, followed by tPA and the fluorogenic plasmin substrate AFC-081. Plasmin generation was monitored at 400 nm excitation and 505 nm emission over 60 minutes.

Blockade of Annexin A2 Reduces Vaso-Obliteration and Neovascularization in the Oxygen-Induced Retinopathy Mouse Model

OIR is a well-characterized, VEGF-driven model of developmental neovascularization.[26] Using this technique, we examined the area of neovascularization in retinas from neonatal mice treated with intravitreal anti-A2 upon release from 75% O_2 (P12) and harvested on P17 (Fig. 4, Fig. 5A). Compared to untreated, control contralateral eyes, we observed significant reductions of 45.97% ± 9 and 37.44% ± 11.8 (SEM) in the NV area in retinas from eyes treated with either 1A7 and 2E6, respectively (see Figs. 4A, 4B, Fig. 5A). We observed a similar significant decrease in eyes treated with anti-VEGF (35.03% ± 8.83 reduction, SEM; see Figs. 4C, 4D, Fig. 5A), with the combination of anti-VEGF and 1A7 (68.64% ± 18.08 reduction, SEM; see Figs. 4E, 4F, Fig. 5A), and with the combination of anti-VEGF and 2E6 (50.41% ± 3.76 reduction, SEM; see Fig. 5A). On the other hand, eyes treated with the

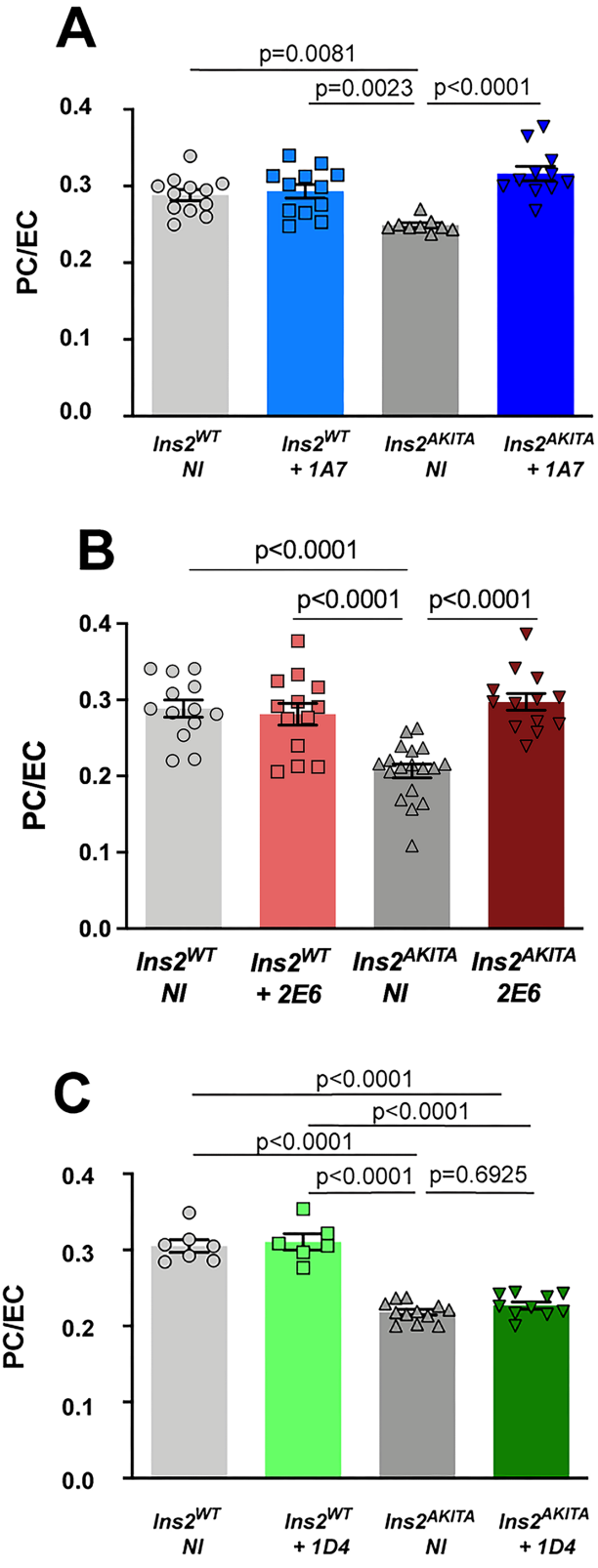

Figure 3. Effect of anti-A2 antibodies on pericyte dropout in diabetic Akita mouse retinas. Mice (Ins^{WT} or Ins^{AKITA}) were treated with anti-A2 IgG 1A7 (**A**), 2E6 (**B**), or control IgG 1D4 (**C**). Four fields (40 times magnification) from a single retina from each of three to five animals were analyzed, each symbol representing one field. Shown are mean values for each group, derived using ANOVA and the Tukey multiple comparisons test, and SEM. NI = non-injected.

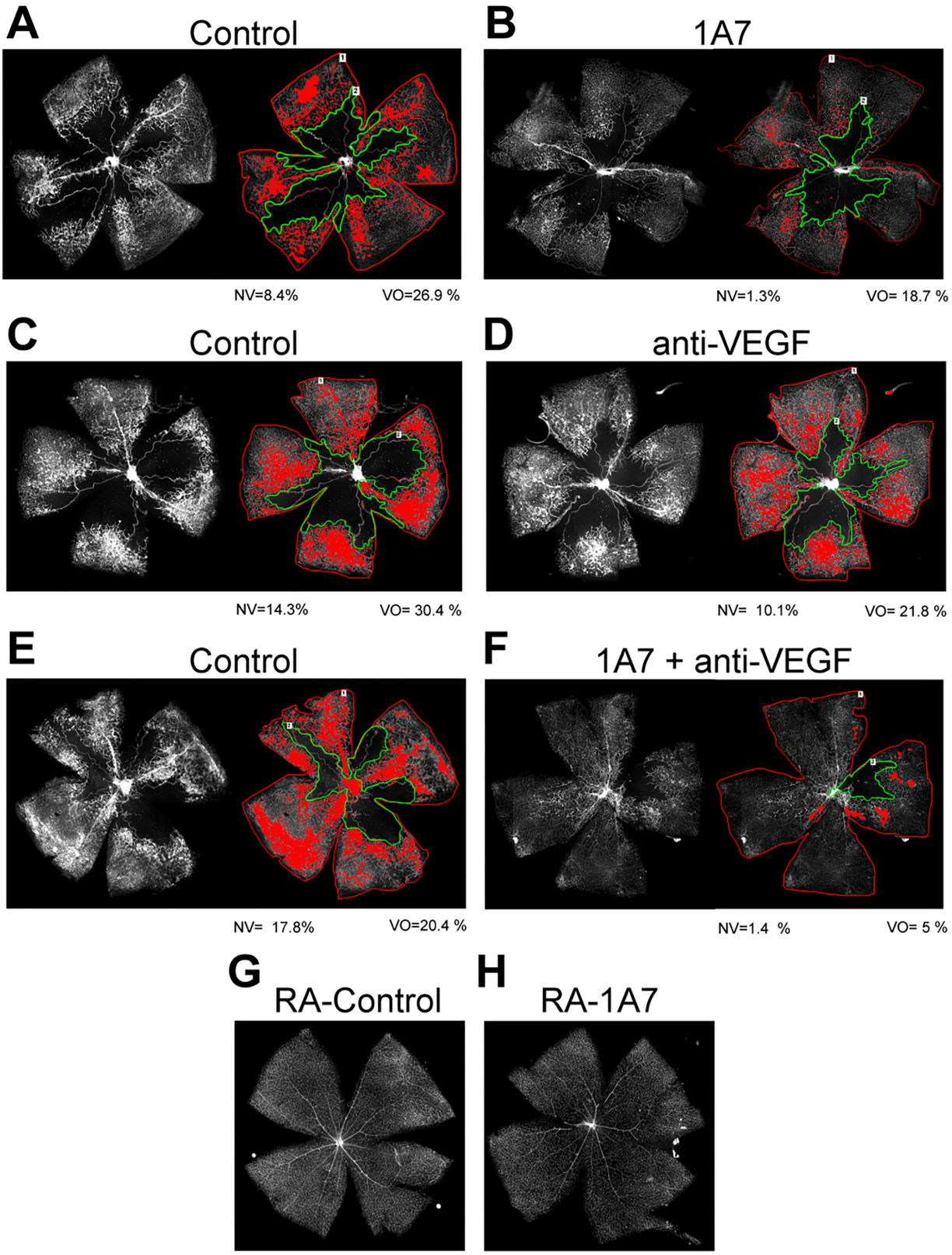

Figure 4. Assessment of retinal neovascularization and vaso-obliteration (VO) in the murine OIR model with and without anti-A2 treatment. Shown are examples of en face preparations of representative retinas from non-injected control eyes (**A, C, E**), as well as contralateral eyes that received intravitreal 1A7 (**B**; 5 µg/mL), anti-VEGF (**D**; 1 mg/mL), or a combination of 1A7 and anti-VEGF (**F**; 5 µg/mL and 1 mg/mL, respectively). NV and VO area, calculated as a percentage of total retinal area as described under Methods, are presented beneath each image. Representative retinas from a P17 mouse maintained in room air, receiving no injection (**G**) or intravitreal 1A7 (**H**; 5 µg/mL), are also shown. The area of VO is encircled in green, and NV area appears in red. Wholemounts were stained with RITC GSL Lectin. Original magnification 10 times, scale bar 500 µm.

Investigative Ophthalmology & Visual Science

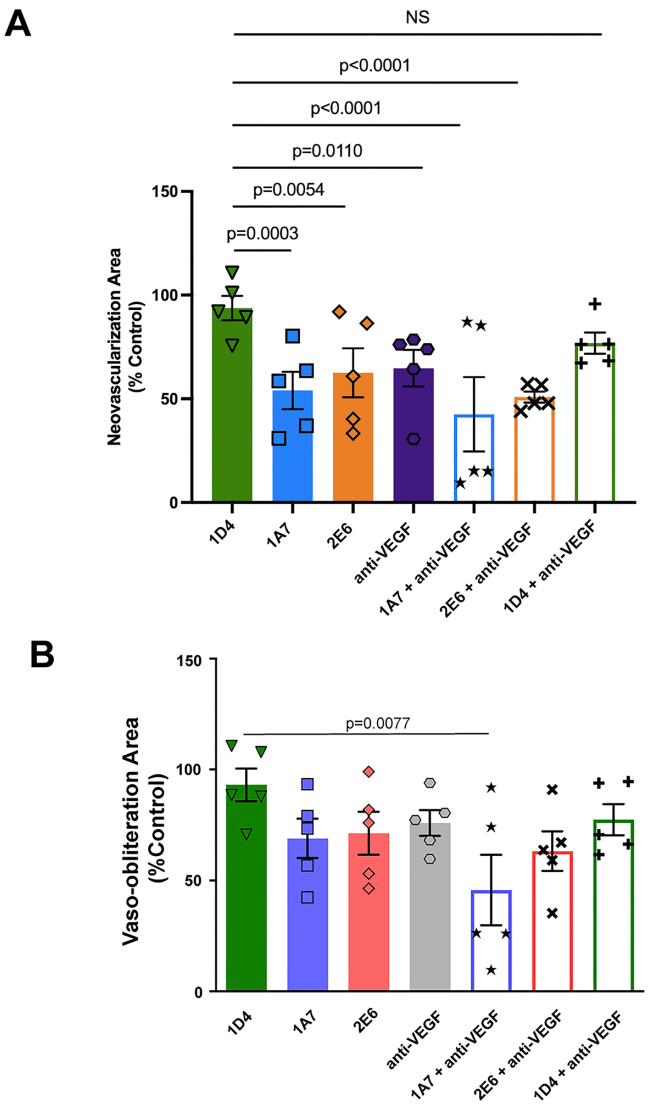

Figure 5. Evaluation of neovascularization and vaso-obliteration (VO) areas in the murine OIR model with and without anti-A2 intervention. NV in treated eyes was calculated as a ratio of total retinal area and expressed as a ratio to NV in untreated eyes (**A**). Similarly, VO in treated eyes was calculated as a ratio of total retinal area and expressed as a ratio VO in untreated eyes (**B**) in P17 oxygen-treated mice. Left eyes were injected with either anti-A2 (1A7 5 µg/mL, and 2E6 15 µg/mL), control antibody (1D4 15 µg/mL), anti-VEGF (1 mg/mL), or a combination of anti-A2 and anti-VEGF. Shown are mean NV or VO areas per section and SEM (n = 5 animals per group). The P values were derived using one-way ANOVA and Dunnett's multiple comparisons test.

control 1D4, showed no change in the NV area (see Fig. 5A). These data indicated that blockade of annexin A2 can reduce the area of neovascularization in the OIR model, and that supplementation with anti-VEGF has an additive effect.

Similarly, we quantified the effect of anti-A2 IgG on post-hyperoxic, retinal VO in neonatal mice treated with anti-A2 upon release from 5 days of 75% O_2 (P12). Comparing retinas from contralateral eyes on P17 (see Figs. 4, 5B), we found a statistically non-significant reduction in VO in eyes treated with anti-A2 (1A7; 31.01% ± 8.87 SEM, or 2E6; 28.71% ± 9.63 SEM) compared to the untreated control (see Figs. 4A, 4B, Fig. 5B). We observed a similar, nonsignificant reduction in the VO area in eyes treated with anti-VEGF (24.38% ± 7.7 SEM; see Figs. 4C, 4D, Fig. 5B). Interestingly, however, the combination of anti-VEGF with 1A7 yielded a highly significant reduction in VO (65.50% ± 13.89 SEM) compared with the 1D4 control (see Figs. 4E, 4F, Fig. 5B). Eyes treated with the non-reactive, control 1D4 showed no change in VO area, and a nonsignificant inhibitory effect when used in combination with anti-VEGF (18.64% ± 7.47 SEM; see Fig. 5B). These data suggest a statistically significant reduction in both VO and NV can be achieved using anti-VEGF in combination with 1A7 (P = 0.0077 and P = 0.0055, respectively), compared to the non-reactive 1D4 without anti-VEGF (see Fig. 5B). These data further suggest that annexin A2 contributes to the depletion of retinal microvessels and subsequent reactive vasoproliferation in this model of DR.

To further evaluate the role of A2 in retinal neovascularization in the OIR model, we enumerated nuclei within NV retinal tufts protruding beyond the nerve fiber layer and into the vitreous (Fig. 6). We found no NV tufts in the retinas of mice maintained in room air, regardless of whether they were injected with anti-A2 (1A7), anti-VEGF, or control antibodies (see Fig. 6A). Under OIR, on the other hand, retinas left untreated showed numerous vascular tufts protruding into the vitreous space (see Fig. 6B). Contralateral retinas injected with 1A7 showed significantly fewer vascular tufts (see Fig. 6B). When NV nuclei were enumerated, we found reductions in tuft nuclei in eyes treated with 1A7 (39.74% ± 6.91 SEM), 2E6 (34.53% ± 6.42 SEM), or anti-VEGF (46.98% ± 13.27 SEM) compared with the non-injected controls (see Fig. 6C). In comparison with the control antibody (1D4, 7.72% ± 9.64 SEM), the combination of anti-VEGF and 1A7 significantly reduced NV tuft formation by 75.14% ± 31.87 SEM (P = 0.0002). The combination of anti-VEGF and 2E6 was statistically significant (65.50% ± 5.31 SEM; reduction; P = 0.0004). These data revealed that the combination of anti-annexin A2 with anti-VEGF can significantly reduce neovascularization in the OIR model.

Because of reports that intravitreal anti-VEGF may enter the systemic circulation in humans possibly causing reduced renal function,[27] hypertension,[28] reduced systemic VEGF,[29] or changes in the fellow eye,[30] we routinely examined the non-injected, contralateral eye by gross appearance and parallel histology in all antibody experiments. In no case have we observed any changes beyond the injected eye.

Annexin A2 Expression Is Elevated in Retinas of Some Patients With Diabetes

Given our findings that expression of annexin A2 contributes to pericyte depletion, as well as vaso-obliteration and NV proliferation in two mouse models of retinopathy, and given our observation that expression of A2 is upregulated in diabetic Akita mice at 3 different ages (statistically significant increase at age 4 months [P = 0.0430] and 6 months [P = 0.0409]; see Supplementary Fig. S4A), we examined annexin A2 expression in postmortem human retinas from subjects reported to have had diabetes. Of note, the mean level of glucose in vitreal fluid harvested from diabetic donor eyes exceeded that of control eyes by almost two-fold (0.27 ± 0.12 mM, n = 6 versus 0.14 ± 0.05 mM, n = 7, mean ± SEM; Supplementary Fig. S5). Overall, immunofluorescence staining of retinal cryosections showed increased A2 expression in the nerve fiber and ganglion cell layers in retinas of diabetic versus non-diabetic subjects (Fig. 7B, a-c, 7A, a-c, respectively). Autofluorescence due to lipofuscin was also present in some sections, such as 7Ac.

Investigative Ophthalmology & Visual Science

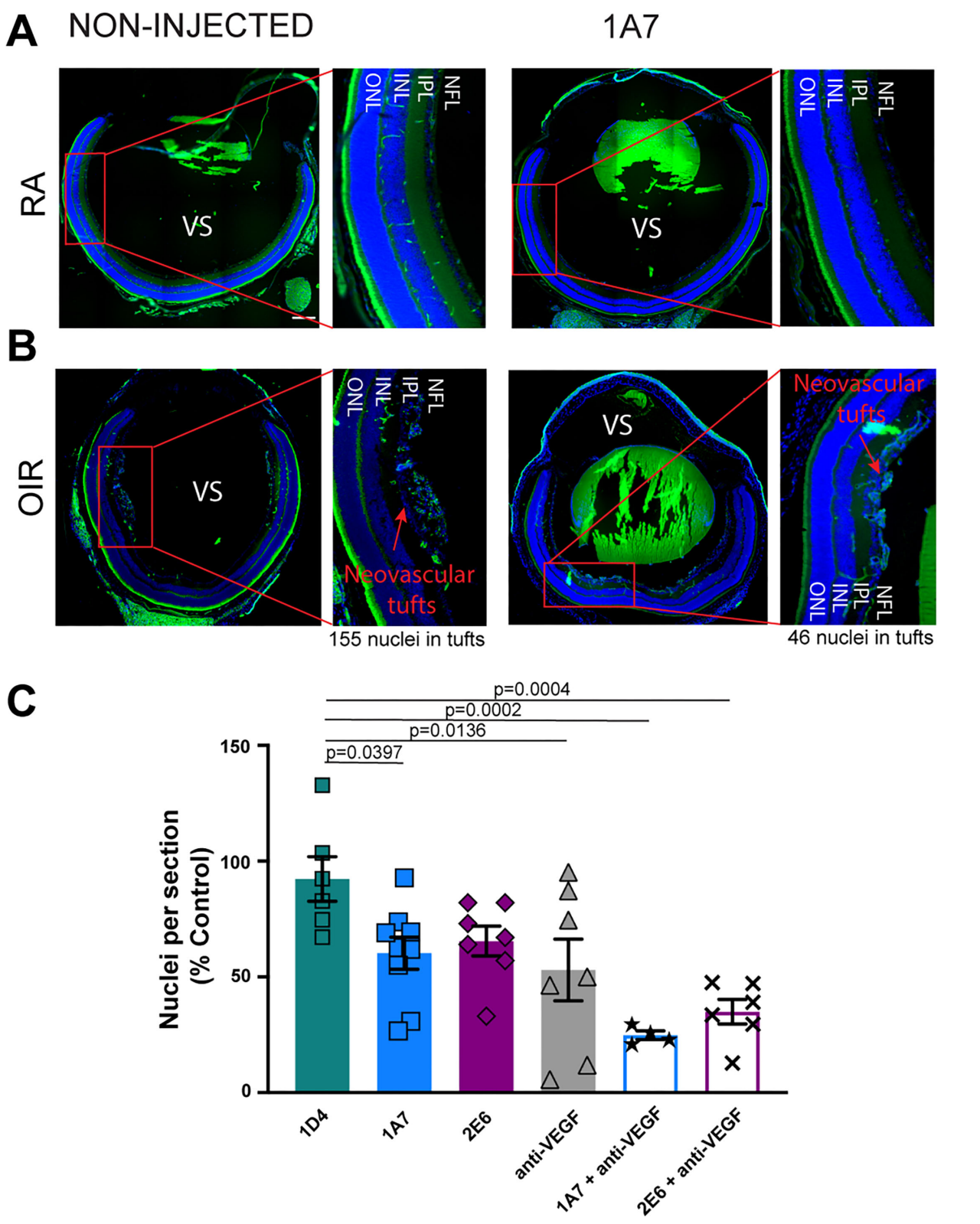

Figure 6. Evaluation of neovascular tuft formation in the murine OIR model with and without anti-A2 intervention. (**A**) Representative sections through the peripheral retinas of P17 mice maintained at room air, and either non-injected or treated with intravitreal anti-A2 (1A7, 5 ug/mL). (**B**) Sections through the peripheral retinal of eyes of P17 mice undergoing OIR, and either non-injected or treated with anti-A2 (1A7, 5 ug/mL). Retinas were stained with rhodamine-conjugated isolectin B4 (*green*) to visualize blood vessels and DAPI (*blue*) to indicate cell nuclei. Scale bar 200 µm. Original magnification 20 times. (**C**) Enumeration of neovascular nuclei in retinal sections from OIR mice treated with anti-A2 (1A7 or 2E6), anti-VEGF IgG, control 1D4, or various combinations thereof. Counts of tuft nuclei in experimental eyes were normalized to those of the non-injected, contralateral eye. Each symbol represents average nuclei per section per eye. Shown are mean counts per group and SEM (n = 4–9 animals per group). The P values were derived using one-way ANOVA and Dunnett's multiple comparisons test.

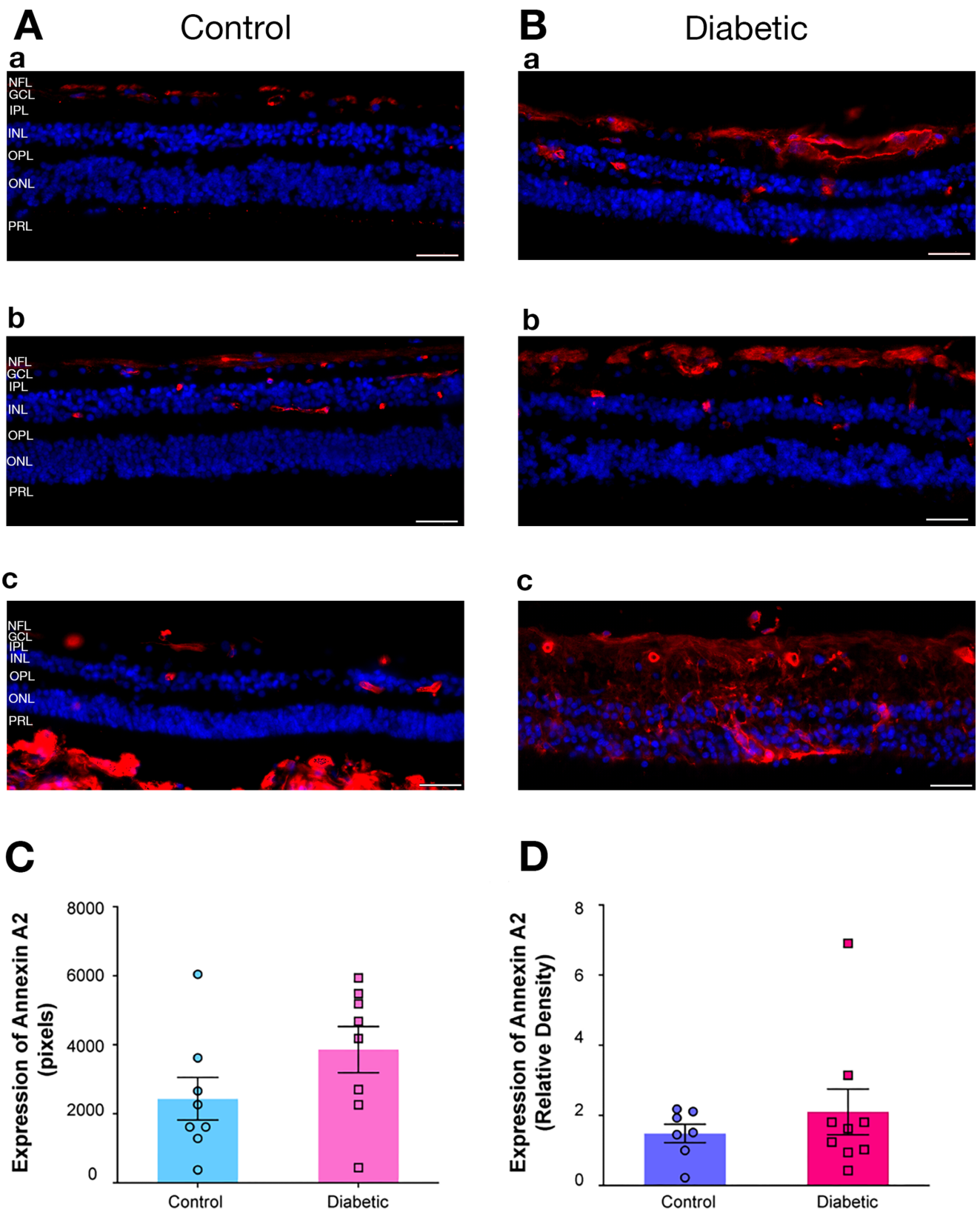

Figure 7. Expression of annexin A2 in retinas of patients with diabetes. Cryosections through retinas isolated from eyes donated postmortem by non-diabetic (**A**) and diabetic (**B**) subjects were stained with anti-annexin A2 followed by secondary IgG, and then DAPI to visualize nuclei. The choroid layer shows autofluorescence due to lipofuscin in some sections (7Ac). Patient ages were 42 to 80 years. Original magnification 20 times. Scale bar 50 µm. (**C**) Expression of annexin A2 (in pixels) quantified in retinal section with NIS Elements software. Each symbol indicates one eye for which up to 17 retinal sections were analyzed. (**D**) A2 protein expression in retinal tissue homogenates from non-diabetic and diabetic subjects by western blot. Each symbol represents one retina. NFL, nerve fiber layer; GCL, ganglion cell layer; IPL, inner plexiform layer; INL, inner nuclear layer; OPL, outer plexiform layer; ONL, outer nuclear layer; PRL, photoreceptor layer.

Investigative Ophthalmology & Visual Science

An example of staining in the absence of primary antibody is displayed in Supplementary Figure S6. Mean A2 expression, calculated as the number of A2-positive pixels occupying the area between the nerve fiber layer (NFL) identified above the ganglion cells layers (GCL) and the inner nuclear layer (INL) was 3860 ± 669 in diabetic samples, and 2436 ± 618 (mean ± SEM, $n = 8$) in controls (Fig. 7C). Furthermore, immunoblot analysis of homogenized retinas from diabetic ($n = 9$) and non-diabetic ($n = 7$) patients also revealed higher overall A2 expression in some subjects, as A2 protein expression averaged 1.48 ± 0.26 arbitrary units (AUs) (mean ± SEM), versus 2.10 ± 0.65 AU (mean ± SEM) in the diabetic group averaged (Fig. 7D). Samples with the 2 highest levels of A2 protein expression (6.90 ± 0.27 AU and 3.14 ± 0.2 AU, respectively) were found in the diabetic group, whereas the highest sample from the non-diabetic group did not exceed a value of 2.20 AU. These data suggest that A2 expression may be upregulated in some diabetic retinas in humans, and suggest a possible role for annexin A2 in human DR.

Discussion

Here, we show for the first time that blockade of annexin A2 can prevent the development of several cardinal features of DR in 2 mouse models. Our data reveal that inhibition of the plasmin-generating action of A2 eliminates the earliest manifestation of DR, namely pericyte dropout, and attenuates later developing features, including vaso-obliteration, neovascularization, and vitreal tuft formation, especially when combined with anti-VEGF, a standard treatment modality. These data could form the basis for a novel treatment approach to DR in humans.

There continues to be an unmet need for safe and effective treatment of DR. Photocoagulation and photodynamic laser ablation of the peripheral retina are traditional therapies that have limited clinical efficacy with respect to improving visual acuity.[31] In addition, untoward effects may include retinal scarring, damage to the choroidal vasculature, and obliteration of the peripheral retina leading to impaired night vision. Although blockade of VEGF has become a standard-of-care for proliferative DR, this approach has additional limitations,[32] including tractional retinal detachment,[33] fluctuations in ocular pressure,[34] and resistance to treatment[35] as well as systemic hypertension and worsening renal disease.[36]

Our previous work suggests that A2 promotes neovascularization in several settings, including the mouse retina and cornea.[10,11,37] Mechanistically, A2 enables activation of plasmin on the surface of vascular endothelial cells, leading to remodeling of fibrin and activation of downstream matrix metalloproteinases[10,11] with degradation of basal membrane and extracellular matrix.[38,39] We, therefore, investigated the effect of anti-A2 neutralizing antibodies in two murine models of DR. We found that either deletion of *Anxa2* or immunologic, functional blockade of A2 prevents pericyte dropout in Akita mice over the first 7 months of life, suggesting that A2-mediated proteolytic activity is likely central to this process. In the OIR model, we found that intravitreal anti-A2 reduced both VO and NV area, and impeded the development of NV tufts. Importantly, head-to-head comparisons of anti-A2 and anti-VEGF showed equivalent effects of the two agents, even though the dose of anti-VEGF was 67 to 200-fold greater.

There is abundant evidence that the annexin A2 system is critical to retinal neoangiogenesis in mice. Upon developing the *Anxa*$^{-/-}$ mouse, we reported fibrin accumulation in all tissues examined, suggesting reduced fibrinolytic activity, as well as a significant reduction in hypoxia-induced neovascularization in the OIR model.[10] We showed further that plasmin-mediated activation of MMPs, known to be important in angiogenic responses, was impaired in tissues from *Anxa2*$^{-/-}$ mice. Third, we demonstrated that vascular endothelial cells isolated from neonatal hearts of *Anxa2*$^{-/-}$ mice demonstrated greatly impaired cell surface-related plasmin generation. In a subsequent paper,[11] we demonstrated that NV in the OIR model required fibrinolytic activity mediated by active plasmin. Evidence for this conclusion included the finding that NV in the wildtype mouse could be blocked by tranexamic acid, which prevents binding of plasminogen to fibrin, thereby inhibiting its activation to plasmin, and leading to fibrin accumulation in response to relative hypoxia. Treatment of OIR mice with ancrod, which depletes fibrinogen and prevents fibrin formation, re-established NV in *Anxa2*$^{-/-}$ mice, indicating that fibrin accumulation in fibrinolysis-impaired *Anxa2*$^{-/-}$ mice blocked new vessel formation. These data established that expression of annexin A2 on the endothelial cell surface is required for robust NV in the neonatal mouse retina, and that absence of A2 prevents the normal fibrinolytic response that supports new vessel outgrowth in this model. Further studies showed that Anxa2 is the product of gene that is upregulated by the action of HIF-1 under hypoxic conditions.[11] An additional study revealed that blockade of tPA binding to A2 upon adduct formation with homocysteine was associated with perivascular fibrin accumulation and inhibition of FGF-induced angiogenesis in the corneal pocket assay.[37] Together, this work has led us to the mechanistic model that absence or blockade of A2 reduces cell surface fibrinolysis by prevented assembly of the A2-tPA-plasminogen complex, and hence plasmin generation, which appears to be necessary for robust neovascularization in the hypoxic retina in mice. The current studies, in which antibodies that block A2-related, tPA-dependent plasmin generation reduce OIR-associated NV, provide further support for this mechanism.

In examining retinas from diabetic human subjects, we noted overexpression of A2 in many samples compared to those from non-diabetic control retinas, using several analytic methods. This finding mirrors the upregulation of A2 in diabetic Akita mice. Immunofluorescence staining of human samples revealed higher numbers of A2-positive retinal blood vessels, many of which penetrate into the inner and outer nuclear layers, as well as anti-A2 immunoreactive material within the nerve fiber and ganglion cell layers. Increased proteolytic activity within the neurovascular unit might impair local blood flow and metabolic activity, by compromising the blood-retina barrier.[40] Accumulation of glutamate is a feature of DR, likely due to Müller cell malfunction,[41] and glutamate appears to stimulate translocation of annexin A2 to the cell surface.[42] Such a pathway could result in increased plasmin generation and subsequent degradation of extracellular matrix. These findings are consistent with our previous observation that A2 is upregulated under hypoxic conditions through the action of HIF-1.[11]

There are several mechanistic pathways whereby the A2 system might promote the vascular changes that characterize DR. Over-expression of A2 might lead to excessive or unopposed plasmin activity, and subsequent degradation

Investigative Ophthalmology & Visual Science

of matrix in which pericytes are embedded. The resulting pericyte dropout could lead to a loss of endothelial cell support with vasodilatation, microaneurysm formation, vascular leak, and endothelial cell apoptosis. Matrix remodeling may also be a result of plasmin-mediated matrix metalloprotease activation. Alternatively, plasmin may release bFGF sequestered within extracellular matrix or attenuate fibrin-mediated endothelial cell adhesion via avb3 integrin.[43] Plasmin may regulate vascular–endothelial cell cadherin-mediated cell self-association[44,45] or signal new programs of gene expression that promote neoangiogenesis.[46,47] Of these possibilities, the first seems most likely, as it conforms most closely to our current understanding of the pathogenesis of DR.

In summary, we have demonstrated here that targeting A2 may be an effective and novel therapeutic approach to retinal neovascularization as occurs in DR, either alone or in combination with anti-VEGF therapy. This approach may be useful in the treatment of other retinal NV disorders, such as retinopathy of prematurity or macular degeneration. Additionally, anti-A2 agents might show efficacy in extra-ocular disorders, such as malignancies, in which tumor growth is dependent upon a growing vascular supply.

Acknowledgments

Support to K.A.H. from the Centers for Therapeutic Innovation (Pfizer Inc.), a Diabetes and Obesity Biologics Science Forum Award (NovoNordisk), the Daedalus Fund for Innovation at Weill Cornell Medicine, the U.S. Army Medical Research and Materiel Command (Grants #W81XWH-14-1-0507 and #W81XWH2110390), and the Belfer Diabetes Fund at Weill Cornell Medicine is gratefully acknowledged.

Disclosure: **V. Dallacasagrande**, None; **W. Liu**, None; **D. Almeida**, None; **M. Luo**, None; **K.A. Hajjar**, None

References

1. Cheung N, Mitchell P, Wong TY. Diabetic retinopathy. *Lancet*. 2011;376:124–136.
2. Teo ZL, Tham YC, Yu M, et al. Global prevalence of diabetic retinopathy and projection of burden through 2045: Systematic review and meta-analysis. *Ophthalmology*. 2021;128:1580–1591.
3. Cho NH, Shaw JE, Karuranga S, et al. IDF diabetes atlas: Global estimates of diabetes prevalence for 2017 and projections for 2045. *Diabetes Res Clin Pract*. 2018;138:271–281.
4. Ahsan H. Diabetic retinopathy–biomolecules and multiple pathophysiology. *Diabetes Metab Syndr*. 2015;9:51–54.
5. Lechner J, O'Leary OE, Stitt AW. The pathology associated with diabetic retinopathy. *Vision Res*. 2017;139:7–14.
6. Semeraro F, Morescalchi F, Cancarini A, Russo A, Rezzola S, Costagliola C. Diabetic retinopathy, a vascular and inflammatory disease: Therapeutic implications. *Diabetes Metab*. 2019;45:517–527.
7. Whitehead M, Wickremasinghe S, Osborne A, Van Wijngaarden P, Martin KR. Diabetic retinopathy: A complex pathophysiology requiring novel therapeutic strategies. *Expert Opin Biol Ther*. 2018;18:1257–1270.
8. Roy S, Kern T, Song B, STuebe C. Mechanistic insights into pathologic changes in the diabetic retina: Implications for targeting diabetic retinopathy. *Am J Pathol*. 2017;187:9–19.
9. McLeod DS, Lefer DJ, Merges C, Lutty GA. Enhanced expression of intracellular adhesion molecule-1 and P-selectin in the diabetic human retina and choroid. *Am J Pathol*. 1995;147:642–653.
10. Ling Q, Jacovina AT, Deora A, et al. Annexin II regulates fibrin homeostasis and neoangiogenesis in vivo. *J Clin Invest*. 2004;113:38–48.
11. Huang B, Deora AB, He K, et al. Hypoxia-inducible factor-1 drives annexin A2 system-mediated perivascular fibrin clearance in oxygen-induced retinopathy in mice. *Blood*. 2011;118:2918–2929.
12. Abu El-Asrar AM, Missotten L, Geboes K. Expression of hypoxia-inducible factor-1alpha and the protein products of its target genes in diabetic fibrovascular epiretinal membranes. *Br J Ophthalmol*. 2007;91:822–826.
13. Lim JI, Spee C, Hinton DR. A comparison of hypoxia-inducible factor-α in surgically excised neovascular membranes of patients with diabetes compared with idiopathic epiretinal membranes in nondiabetic patients. *Retina*. 2010;30:1472–1478.
14. Lima e Silva R, Shen J, Gong YY, et al. Agents that bind annexin A2 suppress ocular neovascularization. *J Cell Physiol*. 2010;225:855–864.
15. Chan CK, Pham LN, Zhou J, Spee C, Ryan SJ, Hinton DR. Differential expression of pro- and antiangiogenic factors in mouse strain-dependent hypoxia-induced retinal neovascularization. *Lab Invest*. 2005;85:721–733.
16. Rohan RM, Fernandez A, Udagawa T, Yuan J, D'Amato RJ. Genetic heterogeneity of angiogenesis in mice. *FASEB J*. 2000;14:871–876.
17. Yoshioka M, Kayo T, Ikeda T, Koizumi A. A novel locus, *Mody4*, distal to D7Mit189 on chromosome 7 determines early-onset NIDDM in nonobese C57Bl/6 (Akita) mutant mice. *Diabetes*. 1997;46:887–894.
18. Wang J, Takeuchi T, Tanaka S, et al. A mutation in the insulin 2 gene induces diabetes with severe pancreatic beta-cell dysfunction in the Mody mouse. *J Clin Invest*. 1999;103:27–37.
19. Barber AJ, Antonetti DA, Kern TS, et al. The Ins2 Akita mouse as a model of early retinal complications in diabetes. *Invest Ophthalmol Vis Sci*. 2005;46:2210–2218.
20. Han Z, Guo J, Conley SM, Naash MI. Retinal angiogenesis in the Ins2 Akita mouse model of diabetic retinopathy. *Invest Ophthalmol Vis Sci*. 2013;54:574–584.
21. Chou JC, Rollins SD, Fawzi AA. Trypsin digest protocol to analyze the retinal vasculature of a mouse model. *J Vis Exp*. 2013;76:e50489–e50495.
22. Connor KM, Krah NM, Dennison RJ, et al. Quantification of oxygen-induced retinopathy in the mouse: A model of vessel loss, vessel regrowth and pathological angiogenesis. *Nat Protoc*. 2009;4:1565–1573.
23. Beltramo E, Porta M. Pericyte loss in diabetic retinopathy: Mechanisms and consequences. *Curr Med Chem*. 2013;20:3218–3225.
24. Hammes HP, Lin J, Renner O, et al. Pericytes and the pathogenesis of diabetic retinopathy. *Diabetes*. 2002;51:3107–3112.
25. Speiser P, Gittelsohn AM, Patz A. Studies on diabetic retinopathy. 3. Influence of diabetes on intramural pericytes. *Arch Ophthalmol*. 1968;80:332–337.
26. Stahl A, Connor KM, Sapieha P, et al. The mouse retina as an angiogenesis model. *Invest Ophthalmol Vis Sci*. 2010;51:2813–2826.
27. Pellé G, Shweke N, Van Huyen J, et al. Systemic and kidney toxicity of intraocular administration of vascular endothelial growth factor inhibitors. *Am J Kidney Dis*. 2011;57:756–759.
28. Fogli S, Del Re M, Rofi E, Posarelli C, Figus M, Danesi R. Clinical pharmacology of intravitreal anti-VEGF drugs. *Eye*. 2018;32:1010–1020.
29. Porta M, Striglia E. Intravitreal anti–VEGF agents and cardiovascular risk. *Int Emerg Med*. 2020;15:199–210.

30. Avery R. What is the evidence for systemic effects of intravitreal anti-VEGF agents, and should we be concerned? *Br J Ophthalmol*. 2014;98:i7–i10.
31. Gibson JM. 25th RCOphth Congress, President's Session paper: 25 years of progress in medical retina. *Eye (Lond)*. 2014;28:1041–1052.
32. Rofagha S, Bhisitkul RB, Boyer DS, Sadda SR, Zhang K. Seven-year outcomes in ranibizumab-treated patients in ANCHOR, MARINA, and HORIZON: A multicenter cohort study (SEVEN-UP). *Ophthalmology*. 2013;120:2292–2299.
33. Torres-Soriano ME, Reyna-Castelán E, Hernández-Rojas M, et al. Tractional retinal detachment after intravitreal injection of bevacizumab in proliferative diabetic retinopathy. *Retin Cases Brief Rep*. 2009;3:70–73.
34. Yonekawa Y, Wu WC, Nitulescu CE, et al. Progressive retinal detachment in infants with retinopathy of prematurity treated with intravitreal bevacizumab or ranibizumab. *Retina*. 2018;38:1079–1083.
35. Sun X, Yang S, Zhao J. Resistance to anti-VEGF therapy in neovascular age-related macular degeneration: A comprehensive review. *Drug Des Devel Ther*. 2016;10:1857–1867.
36. Hanna RM, Barsoum M, Arman F, Selamet U, Hasnain H, Kurtz I. Nephrotoxicity induced by intravitreal vascular endothelial growth factor inhibitors: Emerging evidence. *Kidney Int*. 2019;96:572–580.
37. Jacovina AT, Deora AB, Ling Q, et al. Homocysteine inhibits neoangiogenesis in mice through blockade of annexin A2-dependent fibrinolysis. *J Clin Invest*. 2009;119:3384–3394.
38. Pepper MS. Role of the matrix metalloproteinases and plasminogen activator-plasmin systems in angiogenesis. *Art Thromb Vasc Biol*. 2001;21:1104–1117.
39. Potente M, Gerhardt H, Carmeliet P. Basic and therapeutic aspects of angiogenesis. *Cell*. 2011;146:873–887.
40. Ambati J, Chalam KV, Chawla DK, et al. Elevated gamma-aminobutyric acid, glutamate, and vascular endothelial growth factor levels in the vitreous of patients with proliferative diabetic retinopathy. *Arch Ophthalmol*. 1997;115:1161–1166.
41. Qing L, Puro D. Diabetes-induced dysfunction of the glutamate transporter in retinal Müller cells. *Invest Ophthalmol Vis Sci*. 2002;43:3109–3116.
42. Valapala M, Maji S, Borejdo J, Vishwanatha JK. Cell surface translocation of annexin A2 facilitates glutamate-induced extracellular proteolysis. *J Biol Chem*. 2014;289:15915–15926.
43. Thiagarajan P, Rippon AJ, Farrell DH. Alternative adhesion sites in human fibrinogen for vascular endothelial cells. *Biochemistry*. 1996;35:4169–4175.
44. Bach TL, Barsigian C, Yaen CH, Martinez J. Endothelial cell VE-cadherin functions as a receptor for the beta15-42 sequence of fibrin. *J Biol Chem*. 1998;273:30719–30728.
45. Bach TL, Barsigian C, Chaluppowicz DG, et al. VE-Cadherin mediates endothelial cell capillary tube formation in fibrin and collagen gels. *Exp Cell Res*. 1998;238:324–334.
46. Pendurthi UR, Ngyuen M, Andrade-Gordon P, Petersen LC, Rao LVM. Plasmin induces Cyr61 gene expression in fibroblasts via protease-activated receptor-1 and p44/42 mitogen-activated protein kinase-dependent signalling pathway. *Art Thromb Vasc Biol*. 2002;22:1421–1426.
47. Majumdar M, Tarui T, Shi B, Akakura N, Ruf W, Takada Y. Plasmin-induced migration requires signaling through protease-activated receptor 1 and integrin alpha(9)beta(1). *J Biol Chem*. 2004;279:37528–37534.